ZITA MEDICAL MANAGEMENT

www.hsmc.gr/en/pharmakeftiki-journal/

ΦΑΡΜΑΚΕΥΤΙΚΗ, 38, ΙΙΙ, 2026 | 216-226 ΕΡΕΥΝΗΤΙΚΗ ΕΡΓΑΣΙΑ

PHARMAKEFTIKI, 38, III, 2026 | 216-226 RESEARCH ARTICLE

Synthesis of a Tacrine–Cinnamic Acid Hybrid and Its Chitosan Nanoparticle Formulation for Sustained Release

Haneen Bahjat Al-rubaye[1,3], Qais Abualassal[1]*, Zead Helmi Abudayeh[1], Samer Hasan Hussein-Al-Ali[2], Rami Ayoub[1]

[1]Department of Applied Pharmaceutical Sciences and Clinical Pharmacy, Faculty of Pharmacy, Isra University, Queen Alia International Airport Street, Amman 11622, Jordan
[2] Department of Chemistry, Faculty of Sciences, Isra University, Amman 11622, Jordan
[3] College of Pharmacy, University of Bilad Alrafidain, Diyala, Iraq

https://doi.org/10.60988/p.v38i3.314

ABSTRACT

Tacrine remains a potent acetylcholinesterase inhibitor (AChEI), motivating tacrine-based hybrids and controlled-release formulations for Alzheimer's disease. Here, a tacrine–cinnamic acid hybrid (compound **2**) was synthesized and structurally confirmed by HRMS, ^{1}H-NMR, and ^{13}C-NMR. In vitro AChE inhibition was assessed by Ellman's assay, where compound **2** showed an IC_{50} of 0.735 ± 0.041 μM compared with tacrine (0.00153 ± 0.00015 μM). To develop a delivery system, compound **2** was incorporated into chitosan nanoparticles (CSNPs) via ionic gelation to afford a compound **2**-CSNPs nanocomposite. FTIR and XRD were used to evaluate functional groups and solid-state changes, and TGA was applied to compare thermal behavior of compound **2**, CSNPs, and the nanocomposite. DLS indicated a submicron population with a main intensity peak around 568 nm, while zeta potential measurements showed a negative surface charge (-17 mV). SEM micrographs revealed irregular micrometer-scale agglomerates with a rough, heterogeneous surface and needle/rod-like features. In vitro release at pH 7.4 displayed biphasic behavior, reaching approximately 50% by 400 min and about 80% by 1400 min, indicating sustained release under physiological conditions.

KEYWORDS:
Tacrine; Cholinesterase Inhibitors; chitosan; Drug release, Nanoparticles

ARTICLE INFO:
Received: February 25, 2026
Revised: March 9, 2026
Accepted: March 13, 2026
Available on line: November 2, 2026

*** CORRESPONDING AUTHOR:**
Qais Abualassal,
e-mail: qais.abualassal@iu.edu.jo

1. Introduction

Alzheimer's disease (AD) is the leading cause of dementia and it is one of the major healthcare challenges of our time. The disease is a specific pattern of cognitive and functional decline that occurs with aging and is associated with particular neuropathogenesis which is often accompanied by behavioral disorders such as apathy, aggressiveness and depression[1, 2]. The cholinergic system has a crucial role in AD due to its involvement in cognitive function, memory and learning. The cholinergic hypothesis of AD proposes that deterioration of cholinergic neurotransmission in CNS contributes markedly to cognitive decline associated with this disorder. Most drugs currently used in the treatment of AD are cholinesterase inhibitors; however, they are symptomatic drugs[3]. A wide variety of commercially available drugs and lead compounds used in the treatment of AD contain heterocyclic nuclei which provide privileged physicochemical features[4, 5].

Oxidative stress is a critical factor in the pathogenesis and progression. It refers to an imbalance relating to the formation of reactive oxygen species (ROS) and the brains. Notably, compounds possessing antioxidant activity have demonstrated prospective efficacy for the treatment of AD[6].

Tacrine (Cognex) (Figure 1) was approved by the United States Food and Drug Administration for the treatment of AD in 1993. Although, the clinical use of Cognex was limited because of its hepatotoxicity. Tacrine has, however, remained an important molecule for research into new AD drugs[7].

Considering the multifactorial nature of AD, the traditional agent designed by one-molecule one target approach is insufficient to provide enough befits. Thus, designing compounds that can simultaneously regulate multiple significant targets in the development of AD, has emerged as new strategy. These compounds referred to as multi-target-directed ligands (MTDLs). Novel multifunctional compounds had been designed through linking antioxidants with tacrine, which showed potent activity against different pathologies of AD[8, 9].

Given the growing interest in the development of novel anti-AD drugs, the present work has the scope to synthesize a tacrine derivative, compound **2**, through coupling reaction with antioxidant cinnamic acid as shown in Scheme 1. Compound 2, N-(1,2,3,4-tetrahydroacridin-9-yl)cinnamamide, corresponds to 9-cinnamoylamino-1,2,3,4-tetrahydroacridine disclosed in US Patent 5,175,172; however, full spectral and physicochemical characterization data for this compound were not reported in that patent[10]. To develop a sustained release delivery system, compound **2** was incorporated into chitosan nanoparticles (CSNPs). Chitosan was selected as the carrier polymer because of its biocompatibility, biodegradability, pH-responsive behavior, and suitability for ionic gelation, enabling incorporation of compound **2** into a matrix capable of modulating drug release[11, 12]. in the perspective to have a biologically active compound with AChE inhibitory activity to support the development of a potential lead compound for slowing the progression of Alzheimer's disease.

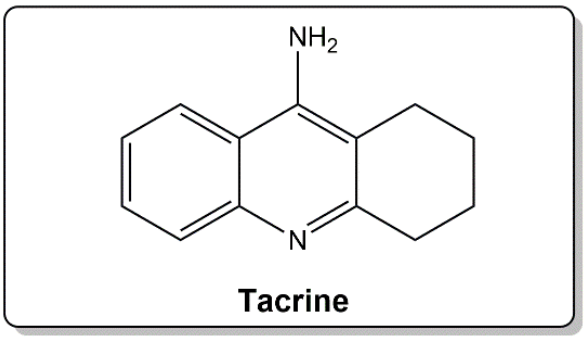
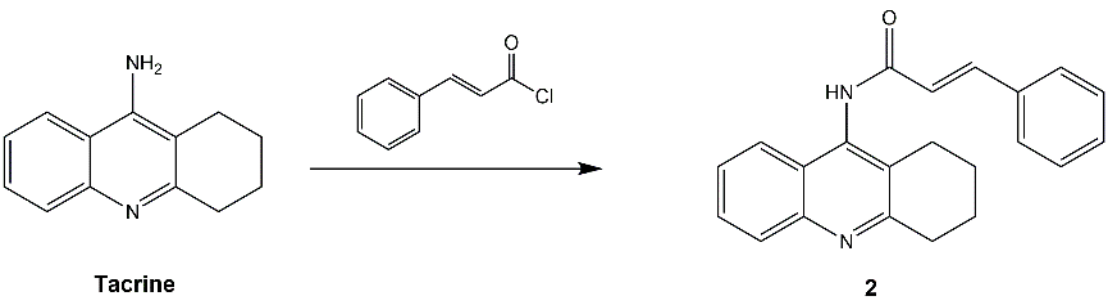


***Figure 1**. Chemical structure of tacrine, the first clinically approved acetylcholinesterase inhibitor for treatment of AD.*

2. Materials and Methods

All chemicals utilized in this work were of analytical reagent grade and used without further purification. CS (low molecular weight, deacetylation 75%–85%) was purchased from Sigma-Aldrich (St. Louis, MO, USA). Sodium tripolyphosphate (TPP)



Scheme 1. *Synthesis of compound* ***2****.*

was purchased from Sigma-Aldrich (St. Louis, MO, USA). 1,2,3,4-tetrahydro-9- acridinamine monohydrochloride ($C_{13}H_{14}N_2$.HCl) was purchased from Cayman Chemicals (Ann Arbor, MI, USA). Acetylthiocholine iodide, Acetylcholinesterase lyophilized powder (electrophorus electricus, electric eel), DTNB {5,5-dithio-bis-(2-nitro benzoic acid)} were purchased from Sigma-Aldrich.

^{1}H- and ^{13}C-NMR spectra were recorded on a Bruker Avance III 500 MHz NMR spectrometer at the Department of Chemistry, Faculty of Science, The University of Jordan, operating at 500 MHz for ^{1}H and 125 MHz for ^{13}C. HRMS analysis was performed using an Apex IV mass spectrometer in positive electrospray ionization mode (ESI^+), Department of Chemistry, Faculty of Science, The University of Jordan. FTIR spectra were recorded at the laboratories of Isra University using a PerkinElmer Spectrum equipped with a UATR Tow accessory, over the range 400–4000 cm^{-1} at a resolution of 4 cm^{-1}. UV-Vis measurements were performed at Isra University using a Thermo Scientific Multiskan GO UV/Vis microplate spectrophotometer (Thermo Fisher Scientific, Waltham, MA, USA).

2.1. Chemical synthesis of N-(1,2,3,4-tetrahydroacridin-9-yl) cinnamamide (2)

Compound **2** was synthesized by heating tacrine monohydrochloride (0.4 g, 1.70 mmol) with cinnamoyl chloride (0.7 g, 4.20 mmol) under solvent free conditions and with continuous stirring overnight at 160 °C. The reaction progress was monitored by TLC. After completion, the reaction mixture was cooled to room temperature and purified by recrystallization from 1-propanol to afford compound **2** as white crystals (0.348 g, 62% yield). Rf = 0.64 ($CHCl_3$/MeOH = 2:1, v/v). HRMS (ESI^+): m/z $[M+H]^+$ found for $C_{22}H_{21}N_2O$, 329.16484. mp 158-160 C°.

^{1}H-NMR (500 MHz, $CDCl_3$): δ = 1.8-3.1 (m, 8H, aliphatic CH_2), 6.84-915 (m, 11H, aromatic/olefinic H), 11.76 (s, 1H, NH).

^{13}C-NMR (125 MHz, $CDCl_3$): δ 164.75 (C=O), 156.29, 152.01, 149.43, 144.12, 136.42, 134.43, 132.72, 130.44, 128.93 (2C), 128.81, 128.52 (2C), 128.01, 125.73, 123.81, 119.67, 29.02, 25.34, 21.11, 20.45.

2.2. Preparation of Chitosan Nanoparticles

A known amount of chitosan was dissolved into 1% (v/v) acetic acid (100 mL) and stirred until the solution became clear. A sodium tripolyphosphate (TPP) solution was prepared dissolving a suitable amount of TPP in distilled water (100 mL). The chitosan nanoparticles (CSNPs) were formed through the addition of TPP solution dropwise to the chitosan solution under continuous stirring until the TPP amount is complete. The pH was adjusted at 5.6 using NaOH (0.5 M). The CSNPs were collected by centrifugation at 4500 rpm and dried overnight in an oven at 40 °C.

2.3. Preparation Compound 2-CSNPs Nanocomposites

The nanocomposite was obtained as a fine pow-

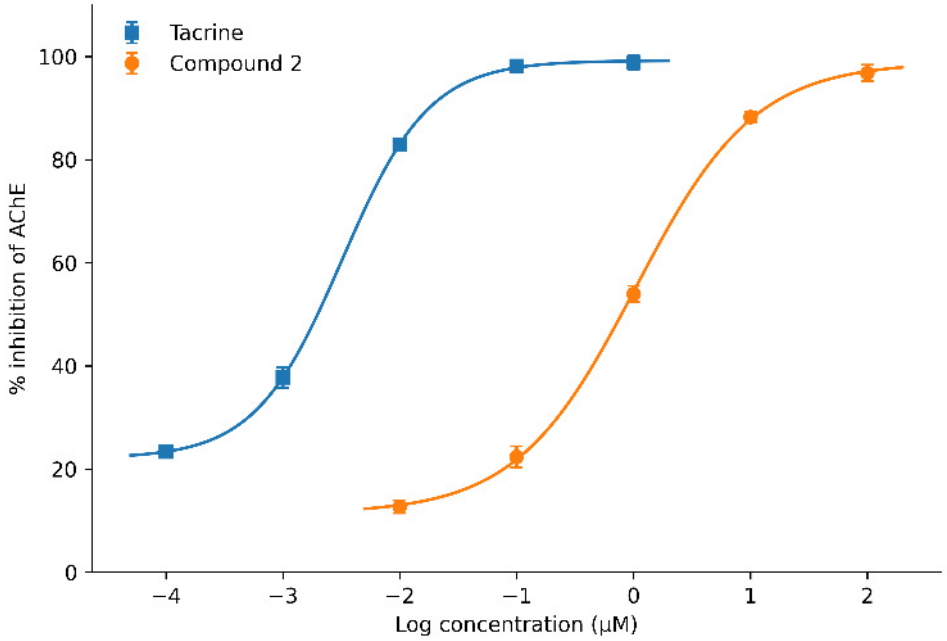


Figure 2. *Concentration–response curves (% inhibition vs log concentration, μM) for tacrine and compound **2** against acetylcholinesterase (AChE), used for IC_{50} determination. Data are presented as mean ± SD (n = 3).*

der. A solution of compound **2** was prepared by dissolving compound **2** in methanol (50 mL). The compound **2** solution was mixed with the chitosan (CS) solution for 1 h, after which a sodium tripolyphosphate (TPP) solution was added dropwise under continuous stirring to form the nanocomposite. The pH of the dispersion was adjusted to 5.6 using 0.5 M NaOH. The mixture was stirred overnight to obtain a homogeneous size distribution and to enhance the loading of compound **2**. The nanocomposite was then collected by centrifugation at 4500 rpm, and the recovered pellet was dried overnight in an oven at 40 °C. The amount of free (unencapsulated) compound **2** in the supernatant was quantified using a UV–Vis spectrophotometer at λmax = 245 nm based on a calibration curve, and the loading efficiency was calculated from the difference between the total amount of compound **2** added and the amount remaining free in the supernatant.

2.4. Determination of AChE Inhibitory Activity Using Ellman's Assay

AChE inhibitory activity was evaluated using the Ellman method with minor modifications. Assays were performed in 96-well plates (final volume 200 μL/well) in Tris-HCl buffer (pH 7.5) containing DTNB (0.4 mM), acetylcholinesterase (final 0.02 U/mL; with 0.1% BSA), and inhibitor solutions prepared in DMSO (final DMSO ≤1% v/v in all wells). After pre-incubation (15 min, room temperature), the reaction was initiated by adding acetylthiocholine iodide (0.4 mM) and incubated for 20 min in the dark; absorbance was read at 412 nm. Vehicle controls (enzyme + DMSO) and blanks (no enzyme) were included, % inhibition was calculated relative to the vehicle control, and IC_{50} values were obtained by nonlinear regression from at least n = 3 independent experiments and reported as mean ± SD.

3. Results and Discussion

3.1. Chemical Synthesis

Compound **2** was prepared via a coupling reaction

Table 1. IC_{50} values (μM) of tacrine and compound **2** against AChE determined by Ellman's assay.

Sample	IC_{50} (μM), mean ±SD
Tacrine	0.00153 ± 0.00015
Compound **2**	0.735 ± 0.041

as shown in Scheme 1[10]. Tacrine was reacted with cinnamoyl chloride under heating in an oil/paraffin bath. The reaction mixture was maintained at 160 °C to initiate product formation and kept to reaction to completion. After cooling, the crude solid was dissolved in hot 1-propanol and filtered to remove insoluble material. The filtrate was concentrated and the product was obtained by recrystallization to afford compound **2** in a good yield (62%) as white crystals. The structure was confirmed by IR, ^{1}H-NMR, ^{13}C-NMR and HRMS.

FTIR spectrum (4000–500 cm^{-1}) of compound **2** showed absorptions consistent with an amide and aromatic system. A strong absorption at 1656 cm^{-1} is attributed to the amide C=O stretching vibration, and showed aromatic C-H stretching at 3095–3048 cm^{-1} and aliphatic C–H stretching at 2934 and 2867 cm^{-1}. A strong band at 1656 cm^{-1} is consistent with an amide C=O, with aromatic/conjugated C=C bands at 1611–1597 cm^{-1}. NMR of compound **2** showed a downfield singlet at δ 11.76 ppm attributable to the amide N-H, while ^{13}C-NMR displayed the amide carbonyl at δ 164.75 ppm.

3.2. Biological Evaluation

The concentrations required to inhibit 50% of AChE activity (IC_{50}) were determined for compound **2** and tacrine. Compound **2** exhibited AChE inhibitory activity with an IC_{50} of 0.735 ± 0.041 μM (Table 1).

Compound **2** showed a concentration-dependent inhibition of AChE in Ellman's assay (Figure 2). Ta-

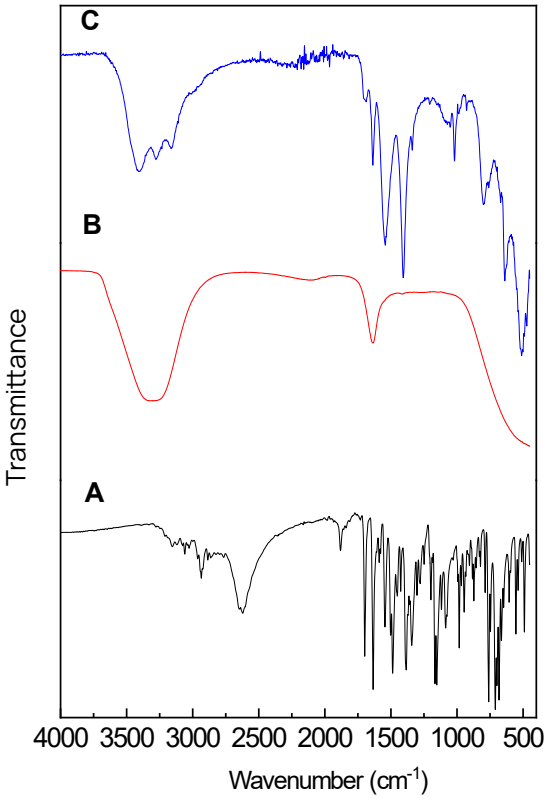


***Figure 3**. FTIR spectra of (A) compound 2, (B) chitosan nanoparticles (CSNPs), and (C) compound 2–CSNPs nanocomposite.*

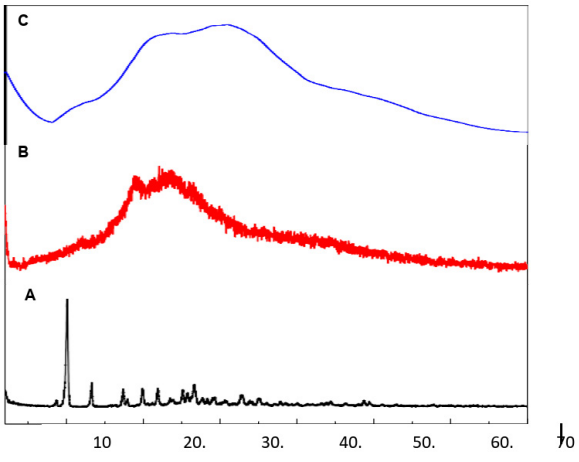


Figure 4. *XRD diffraction spectra of compound **2** (A), CSNPs (B) and Compound **2**-CSNPs nanocomposites (C).*

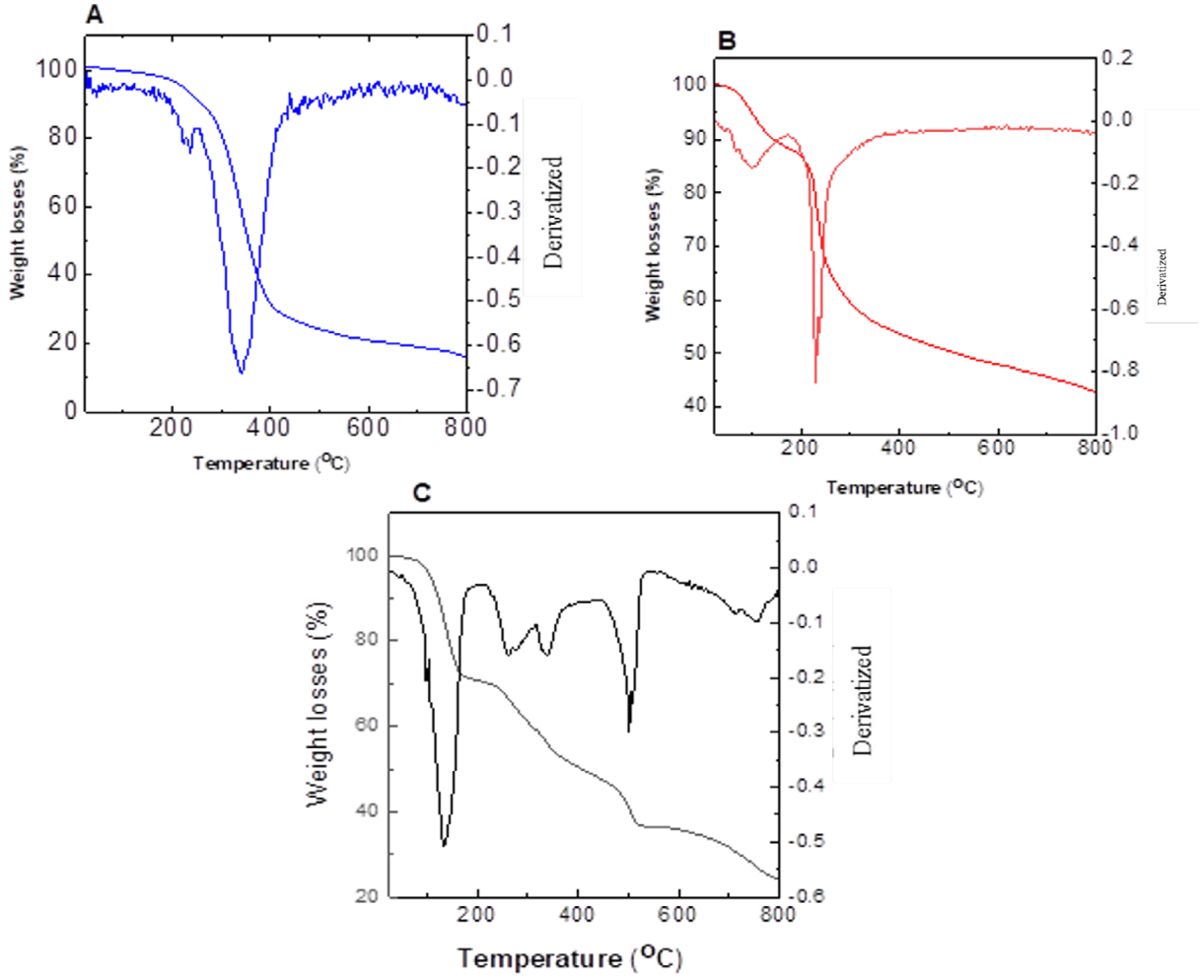


Figure 5. *TGA thermograms of (A) compound **2**, (B) chitosan nanoparticles (CSNPs), (C) compound **2**-CSNPs nanocomposite.*

crine was used as a reference inhibitor and exhibited markedly higher potency, achieving comparable inhibition at much lower concentrations, consistent with its lower IC_{50} value. Data are presented as mean ± SEM (n = 3). IC_{50} values were estimated from the inhibition–concentration (log_{10}) relationship using Microsoft Excel (Figure 2). Statistical comparisons were performed using a t-test, with $p \leq 0.05$ considered significant.

3.3. Characterization of Nanocomposite

Chitosan is a pH-sensitive polymer due to protonation of its amine groups ($pK_a = 6.5$). The pH of the prepared chitosan solution was 5.63, which favors protonation and electrostatic interactions necessary

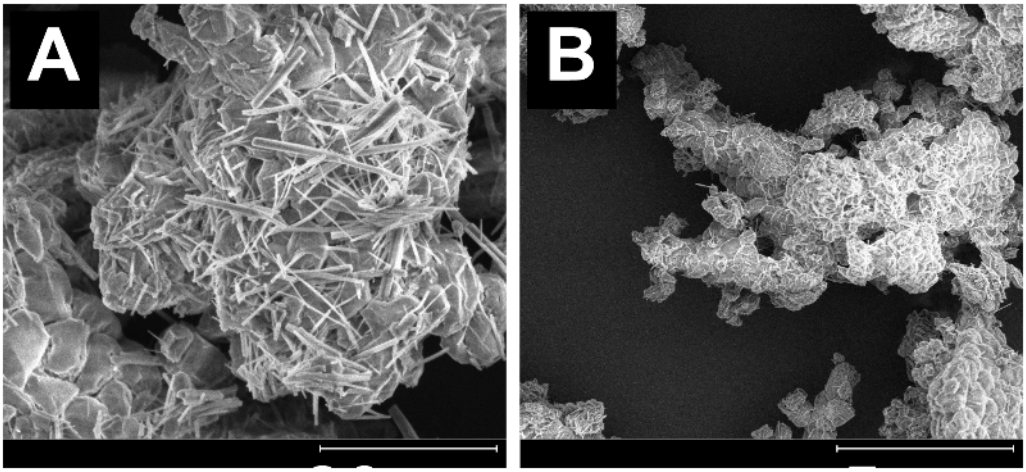


Figure 6. *SEM micrographs of compound **2**-loaded chitosan nanoparticles at different magnifications: (A) 20,000×, scale bar = 5 μm; (B) 5,000×, scale bar = 20 μm.*

for nanoparticle formation and complexation[11,21].

FTIR spectra (Figure 3) were recorded for compound **2**, CSNPs, and compound **2**-CSNPs. Compound **2** showed characteristic bands in the amide/aromatic regions, while CSNPs exhibited a broad band in the 3200–3500 cm^{-1} region attributed to overlapped O-H/N-H stretching and bands in the 1650–1590 cm^{-1} region consistent with amide/NH_2 vibrations. After loading, the composite spectrum showed noticeable changes in the amide/aromatic regions and attenuation/overlap of characteristic compound **2** bands, supporting successful incorporation of compound **2** into the CSNP matrix.

3.4. X-Ray Diffraction

X-ray diffraction (XRD) was used to evaluate the crystallinity of the polymeric nanoparticles and the nanocomposite. Figure 4 shows the XRD patterns of compound **2** (A), CSNPs (B), and compound **2**-CSNPs (C). The diffractogram of compound **2** (2θ = 2-70°) exhibited multiple sharp diffraction peaks at 2θ = 10.18°, 13.85°, 18.20°, 20.10°, 21.38°, 24.20°, 29.20°, 34.36°, and 34.90°, indicating a crystalline structure. In contrast, the XRD pattern of CSNPs showed a broad halo with the absence of sharp reflections, consistent with a predominantly amorphous nature. A similar broad pattern was observed for the compound **2**-CSNPs nanocomposite, with marked reduction of the characteristic crystalline peaks of compound **2**, suggesting decreased crystallinity after incorporation into the chitosan matrix. The reduction in chitosan crystallinity can be attributed to ionic crosslinking with TPP, which disrupts chain packing and promotes formation of the nanoparticulate structure [15].

3.5. Thermogravimetric analysis (TGA)

Thermogravimetric analysis (TGA) was used to evaluate the thermal behavior of compound **2**, CSNPs, and the compound **2**-CSNPs nanocomposite (Figure 5). Compound **2** exhibited a major degradation event at higher temperature (maximum around 350 °C), indicating thermal decomposition with a measurable residual mass at 800 °C. CSNPs showed multistep degradation, including an initial weight decrease below 150 °C attributed to loss of adsorbed water, followed by a main degradation step around 200-300 °C range associated with decomposition of the chitosan polymer backbone. The compound 2-CSNPs nanocomposite displayed a similar multistep profile; however, changes in the positions and/or intensities of the degradation steps and the resid-

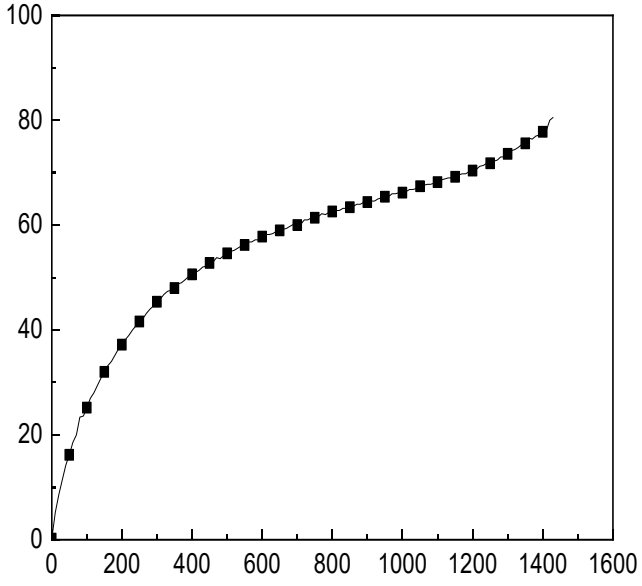


Figure 7. *Cumulative release profile of compound **2** from compound **2**-CSNPs nanocomposite in phosphate buffer*.

ual mass compared with CSNPs suggest interactions between compound **2** and the chitosan matrix and the effect of ionic crosslinking with TPP, which can modify chain packing and thermal stability[16,21].

3.6 Scanning Electron Microscopy (SEM)

SEM micrographs were used to examine the surface morphology of the compound **2**-CSNPs nanocomposite and recorded at 5000× and 20,000× magnification (Figure 6). The images show irregular, micrometer-scale agglomerates with a rough, heterogeneous surface, containing needle/rod-like features along with plate/flake-like fragments. The sample appears polydisperse, with evident clumping and clustering, indicating aggregation of the nanocomposite during/after drying[17,18].

3.7. In vitro Release Study of 2-Nanocomposites

The cumulative release profile of compound **2** from the compound **2**-CSNPs nanocomposite at pH 7.4 is shown in Figure 7. The release exhibited a biphasic behavior. An initial faster release phase was observed, reaching approximately 50% within approximately 400 minutes, which may be attributed to drug molecules located near the particle surface or weakly associated with the polymeric matrix. This was followed by a slower, sustained release phase, with cumulative release gradually increasing to about 80% at approximately 1400 minutes. Overall, the compound **2**-CSNPs formulation demonstrated a sustained-release behavior under physiological pH conditions. The observed

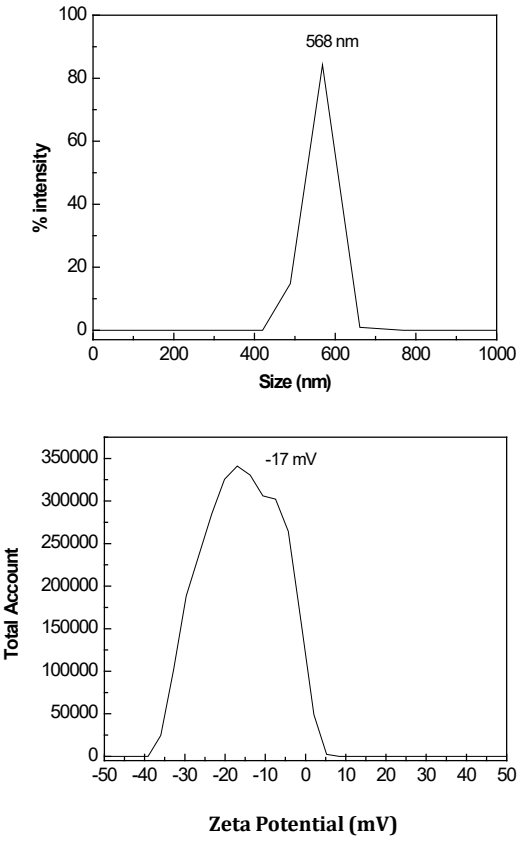


Figure 8. *(A) DLS intensity-weighted particle size distribution of the compound **2**-CSNPs nanocomposite. (B) Zeta potential distribution of the compound **2**-CSNPs nanocomposite.*

biphasic release pattern can be consistent with chitosan-based delivery systems reported in the literature previously. The initial burst phase is commonly attributed to surface-associated dug release, whereas the subsequent slower phase reflects diffusion through the hydrated polymeric network, together with swelling of the chitosan matrix and gradual structural relaxation. In ionically crosslinked chitosan systems, the extent of release is additionally influenced by the degree of TPP crosslinking, medium penetration, and pH-dependent polymer hydration[17,20].

The release mechanism is commonly governed by a combination of diffusion of the drug through the hydrated polymer network, and polymer swelling and/or gradual matrix erosion. For chitosan-based nanocomposites, penetration of the aqueous medium leads to polymer hydration and swelling, which can generate diffusion pathways and facilitate the outward diffusion of encapsulated compound **2**. The rate of release can also be influenced by the degree of ionic crosslinking, water uptake, and environmental conditions like pH [19,21].

3.8. Particle Size and Zeta Potential

The hydrodynamic particle size distribution of the compound **2**-CSNPs nanocomposite was measured at 25 °C by dynamic light scattering (DLS) using a Malvern Zetasizer Nano ZS (Malvern Instruments, Malvern, UK). As shown in Figure 8A, the sample exhibited a main intensity-weighted size peak centered at approximately 568 nm, consistent with the presence of submicron particles and/or aggregated populations in suspension. Zeta potential (ζ) was determined at 25 °C using the same instrument by electrophoretic light scattering (ELS). The nanocomposite showed a ζ-potential of approximately -17 mV (Figure 8B), indicating a negatively charged surface and limited-to-moderate electrostatic stabilization. Such ζ values can reduce aggregation to some extent, although some clustering may still occur depending on pH and ionic strength.

4. Conclusion

In this study, a tacrine-cinnamic acid hybrid (compound **2**) was synthesized as a potential lead for Alzheimer's disease (AD). Compound 2 showed inhibitory activity against acetylcholinesterase (AChE) in vitro using Ellman's assay with potential antioxidant properties. The structure of compound **2** was confirmed using HRMS, ^{1}H-NMR, and ^{13}C-NMR. To develop a delivery system, compound **2** was incorporated into chitosan nanoparticles (CSNPs) to form a compound **2**-CSNPs nanocomposite by ionic gelation. FTIR and XRD were used to characterize the nanocomposite and assess interactions/solid-state changes. In vitro release testing indicated a sustained-release profile of compound **2** from the nanocomposite. Overall, the results support compound **2**-CSNPs as a chitosan-based formulation for controlled delivery of compound **2**.

Declaration of conflicting interests: The authors report no conflicts of interest in this work.

Acknowledgement: The authors would like to thank the Faculty of Pharmacy at Isra University for providing funding for this research.

References

1. Haughey N.J., Bandaru V.V., Bae M., Mattson M.P. Roles for dysfunctional sphingolipid metabolism in Alzheimer's disease neuropathogenesis. *Biochim. Biophys. Acta*. 1801(8), 878-86, 2010. doi: 10.1016/j.bbalip.2010.05.003
2. Huang Y.Y., Gan Y.H., Yang L., Cheng W., Yu J.T. Depression in Alzheimer's Disease: Epidemiology, Mechanisms, and Treatment. *Biol. Psychiatry*. 95(11), 992-1005, 2024. doi: 10.1016/j.biopsych.2023.10.008
3. Chen Z.R, Huang J.B, Yang S.L, Hong F.F. Role of Cholinergic Signaling in Alzheimer's Disease. *Molecules*. 27(6), 1816, 2022. doi: 10.3390/molecules27061816
4. Abualassal Q., Abudayeh Z., Sirhan A., Mkia A. Exploring Quinazoline as a Scaffold for Developing Novel Therapeutics in Alzheimer's Disease. *Molecules*. 30(3), 555, 2025. doi: 10.3390/molecules30030555
5. Sánchez J.D., Alcántara A.R., González J.F., Sánchez-Montero J.M. Advances in the discovery of heterocyclic-based drugs against Alzheimer's disease. *Expert Opin. Drug Discov*. 18(12), 1413-1428, 2023. doi: 10.1080/17460441.2023.2264766
6. Bartra C., Yuan Y., Vuraić K., Valdés-Quiroz H., Garcia-Baucells P., Slevin M., Pastorello Y., Suñol C., Sanfeliu C. Resveratrol Activates Antioxidant Protective Mechanisms in Cellular Models of Alzheimer's Disease Inflammation. *Antioxidants (Basel).* 13(2), 177, 2024. doi: 10.3390/antiox13020177
7. Summers W.K. Tacrine (THA, Cognex®). *J. Alzheimers Dis*. 2(2), 85-93, 2000. doi:10.3233/JAD-2000-2204
8. Chen Y., Zhu J., Mo J., Yang H., Jiang X., Lin H., Gu K., Pei Y., Wu L., Tan R., Hou J., Chen J., Lv Y., Bian Y., Sun H. Synthesis and bioevaluation of new tacrine-cinnamic acid hybrids as cholinesterase inhibitors against Alzheimer's disease. *J. Enzyme Inhib. Med. Chem*. 33, 290-302, 2018. doi: 10.1080/14756366.2017.1412314
9. Oset-Gasque M.J., Marco-Contelles J.L. Tacrine-Natural-Product Hybrids for Alzheimer's Disease Therapy. *Curr. Med. Chem*. 27, 4392-4400, 2020. doi: 10.2174/0929867325666180403151725
10. Fredj D., Dietlin F. Method of Alleviating AIDS Symptoms and Compositions Therefor. US Patent 5, 175, 172, 1992.
11. Rahimi S., Khoee S., Ghandi M. Preparation and characterization of rod-like chitosan-quinoline nanoparticles as pH-responsive nanocarriers for quercetin delivery. *Int. J. Biol. Macromol*. 128, 279-289, 2019. doi: 10.1016/j.ijbiomac.2019.01.137
12. Mohammed M.A., Syeda J.T.M., Wasan K.M., Wasan E.K. An Overview of Chitosan Nanoparticles and Its Application in Non-Parenteral Drug Delivery. *Pharmaceutics*. 9(4), 53, 2017. doi: 10.3390/pharmaceutics9040053
13. Lanigan R.M., Sheppard T.D. Recent developments in amide synthesis: Direct amidation of carboxylic acids and transamidation reactions. *Eur. J. Org. Chem*. 33, 7453-7465, 2013.
14. Ellman G.L., Courtney K.D., Andres V.Jr., Featherstone R.M. A new and rapid colorimetric determination of acetylcholinesterase activity. Biochem. Pharmacol. 7, 88-95, 1961.
15. Grenha A. Chitosan nanoparticles: a survey of preparation methods. *J. Drug Target*. 20, 291-300, 2012. doi: 10.3109/1061186X.2011.654121
16. Hussein-Al-Ali S., Kura A., Hussein M.Z., Fakurazi S. Preparation of chitosan nanoparticles as a drug delivery system for perindopril erbumine. *Polym. Compos*. 39, 544-552, 2018. doi. org/10.1002/pc.23967
17. Lazaridou M., Christodoulou E., Nerantzaki M., Kostoglou M., Lambropoulou D.A., Katsarou A., Pantopoulos K., Bikiaris D.N. Formulation and In-Vitro Characterization of Chitosan-Nanoparticles Loaded with the Iron Chelator Deferoxamine Mesylate (DFO). *Pharmaceutics*. 12(3), 238, 2020. doi: 10.3390/pharmaceutics12030238
18. Alehosseini E., Shahiri Tabarestani H., Kharazmi M.S, Jafari S.M. Physicochemical, Thermal, and Morphological Properties of Chitosan Nanoparticles Produced by Ionic Gelation. *Foods*. 11(23),

3841, 2022. doi: 10.3390/foods11233841

19. Milenkova S., Ambrus R., Mukhtar M., Pilicheva B., Marudova M. Spray-Dried Chitosan Hydrogel Particles as a Potential Delivery System for Benzydamine Hydrochloride. *Gels.* 10, 189, 2024. doi: 10.3390/gels10030189
20. Anju A.B., Gopal K.S., Panchami P.S., Vijayaraghavan R. A simple and user-friendly protocol for chitosan nanoparticle synthesis. *Discov. Nano*. 20, 211, 2025. doi.org/10.1186/s11671-025-04406-4
21. Bhumkar D.R, Pokharkar V.B. Studies on effect of pH on cross-linking of chitosan with sodium tripolyphosphate: a technical note. *AAPS PharmSciTech.* 7, 50, 2006. doi: 10.1208/pt070250